Journal of Alloys and Compounds 504 (2010) 357–361

Contents lists available at ScienceDirect

Journal of Alloys and Compounds

journal homepage: www.elsevier.com/locate/jallcom

Thermal stability of cerium-based bulk metallic glasses. Influence of iron addition

Q. Wang [a,b], J.M. Pelletier [c,*], J.J. Blandin [b]

[a] Institute of Material Science, 200072 Shanghai University, PR China
[b] Grenoble-INP, SIMAP-GPM2, CNRS, 38042 Saint-Martin d'Hères, France
[c] Université de Lyon, Mateis, UMR CNRS 5510, Bat. B. Pascal, INSA-Lyon, 69621 Villeurbanne Cedex, France

ARTICLE INFO

Article history:
Received 4 December 2009
Accepted 19 May 2010
Available online 31 May 2010

Keywords:
Ce-based bulk metallic glass
Crystallization
X-ray diffraction
Dynamic mechanical analysis

ABSTRACT

Cerium-based bulk metallic glasses are attractive due to their low glass transition temperature, comparable to that of polymers. Their mechanical properties, especially their elastic and viscoelastic ones are reported in a large temperature range. Like in other bulk metallic glasses, the shear modulus, close to 11.5 GPa at room temperature, decreases drastically in the glass temperature range (at about 373 K), while the viscoelastic component becomes very important. Heating to high temperature induces crystallization. As shown by X-ray diffraction experiments performed in situ, the increase of elastic modulus due to the formation of crystalline particles is strongly connected to the volume fraction of these particles. Addition of iron shifts the phenomena towards higher temperatures and affects the crystallization process.

1. Introduction

Manufacturing of bulk metallic glasses has now become fairly usual with the fabrication in the past decade of several families of extremely good glass forming multicomponents alloys, especially those based on conventional metal transition metals (Zr, Pd, Fe, Ti, Cu). More recently, in 2004, rare earth based BMG have been developed and among them, cerium-based alloys are probably the most promising ones [1–5]. First, cerium is the most abundant rare earth metal. But the most attractive feature is its very low glass transition temperature. For instance in Ce–Cu–Al alloys, T_g may be lower than 100 °C and therefore they can be easily processed for instance in boiling water [4,5]. This low T_g may be compared to that of common polymers. However, if polymers are less expensive and more easy to prepare, they are non-conductive materials and their Young modulus at ambient temperature are lower than that of cerium-based BMG, typically one decade lower.

Cerium-based BMG have been the subject of various investigations [1–5], especially by DSC, in order to determine their characteristic temperatures: T_g (glass transition temperature), and T_x (onset of crystallization). The influence of the chemical composition on such temperatures has also been reported. It is well known [6] that minor additions can play a major role, for instance on the glass forming ability. They favor the formation of atomic dense configurations and liquid with a high viscosity. So, thermodynamically, these minor additions make the liquid energetically closer to the crystalline state and, cinematically, they make the melt more viscous which leads to slow crystallization kinetics. Such additions can also purify the melt and consequently to limit the possibility of heterogeneous crystallization during cooling or during a further annealing. In cerium-based BMG, Fe is the most common addition element used [7].

Concerning the mechanical properties of Ce-based BMG, reported investigations address elastic and plastic behavior [8–10]. An anomalous temperature dependence of the elastic properties [9] has been observed: although the young modulus (E) and the shear modulus (G) display softening mode with decreasing temperature, the bulk modulus (B) abnormally decreases with decreasing temperature below room temperature. This result was attributed to the specific electronic configuration of cerium. However, many questions have not been addressed: (i) What is the influence of temperature of the mechanical properties of cerium-based BMG above the room temperature? (ii) It is well known that in amorphous materials, in addition to elasticity and plasticity, a viscoelastic component exists, with a magnitude which may be very large in the supercooled liquid region [11–21]. What's about cerium-based materials? (iii) What is the influence of Fe on the crystallization behavior?

So, the aim of the present work is to give some answers to these different questions.

2. Experimental procedure

Amorphous plates, with a thickness of 1 mm, of $(Ce_{0.72}–Ce_{0.28})_{90-x}–Al_{10}–Fe_x$ ($x = 0\%$, 5% or 10%) have been prepared in Shanghai University, China, by rapid quenching of the melts into a cooled copper mold under argon atmosphere.

---

* Corresponding author. Tel.: +33 4 72 43 83 18; fax: +33 4 72 43 85 28.
E-mail address: jean-marc.pelletier@insa-lyon.fr (J.M. Pelletier).

0925-8388/$ – see front matter © 2010 Elsevier B.V. All rights reserved.
doi:10.1016/j.jallcom.2010.05.070

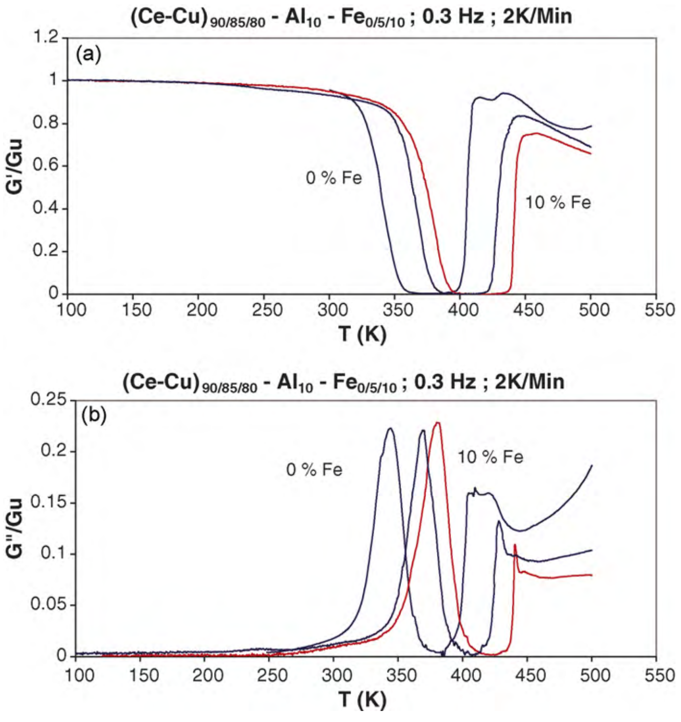

Fig. 1. Dependence of the normalized shear modulus of $(\mathrm{Ce{-}Cu})_{90-x}{-}\mathrm{Al}_{10}\mathrm{Fe}_x$ ($x = 0\%$, 5% or 10%) as a function of temperature. G_u is the unrelaxed shear modulus. The measurement frequency is 0.3 Hz. The heating rate is 3 K/min. (a) Storage modulus and (b) loss modulus.

Wide X-ray scattering on the section of the sample, using a Cu-Kα radiation was conducted in a large temperature range, from 100 to 550 K, either during isothermal treatment or during continuous heating (at 1 K/min).

The final samples for dynamic mechanical (DMA) experiments were cut by electric discharge from the plates and they had dimensions of approximately 1 mm thickness, 3 mm width and 30 mm length. Glass transition temperature (T_g) and onset of the crystallization temperature T_x, have been determined by using a differential scanning calorimeter DSC7 (PerkinElmer). The shear dynamic measurements (i.e. DMA) have been carried out using a home-made specific device [22]. Frequency range is 10^{-4} to 1 Hz. In the present study, a sinusoidal shear stress was applied and the corresponding shear deformation was recorded. Strain amplitude was lower 10^{-4}. In a first step, experiments were performed at a given frequency during continuous heating at 1 K/min, 2 K/min or 3 K/min between 100 and 600 K. Then, in a second step, measurements were performed at a fixed temperature, but for different frequencies. Measurements started with the lowest temperature and highest frequency. According to the experimental procedure defined by Schröter et al. [18], after performing all the experimental measurements, the run with the first temperature was repeated to check that no crystallization occurred. All the DMA experiments have been performed under helium atmosphere.

3. Experimental results and discussion

3.1. Evolution of the complex dynamic shear modulus during a continuous heating

Fig. 1 shows the temperature dependence of the storage (G') and the loss (G'') dynamic shear modulus, observed during an heating with a testing frequency of 0.3 Hz. G_u is the unrelaxed modulus, i.e. in the present experimental conditions, the modulus at 100 K, since then G'' is negligible. G_u increases from 11.5 GPa to 14.0 GPa, where the iron content increases from 0 to 10%. Curves for the different compositions are similar, but the presence of iron induces a shift towards higher temperatures. The variation of G' with temperature occurs in several stages. A rapid decrease of G' is observed, associated with a large increase of G''. A maximum of G'' appears at a temperature called T_α. This phenomenon, which is observed in all the amorphous materials, is generally referred to the main (or α relaxation) and is associated to the dynamic glass transition process. Let us mention that T_α, which depends on the testing frequency (see below) is different from the calorimetric glass transition temperature T_g.

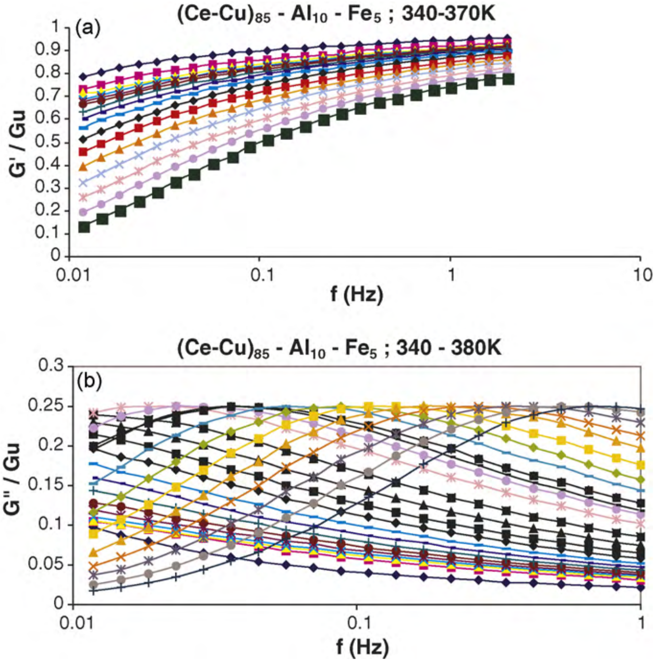

Fig. 2. Dependence of the normalized shear modulus of $(\mathrm{Ce{-}Cu})_{90-x}{-}\mathrm{Al}_{10}\mathrm{Fe}_x$ as a function of frequency at different temperatures. (a) Storage modulus and (b) loss modulus.

For higher temperatures a plateau of G' is observed and then a large increase of G' appears, which corresponds to the crystallization phenomenon of the supercooled liquid. One can note that this process is abrupt. After this important increase in G', a continuous moderate decrease is observed as in any crystalline material. However, this final decrease may be more or less regular: in the alloy without iron different steps can be observed, while the presence of iron atoms seems to induce a more uniform evolution. These observations suggest that the iron content in the studied Ce-based metallic glasses influences the crystallization process. X-ray diffraction experiments have to be carried out to investigate this point in more details (see Section 3).

3.2. Influence of testing frequency during isothermal measurements on complex dynamic shear modulus

The α relaxation is a thermo-mechanically activated phenomenon. Indeed its features depend on testing frequency [10–19]. Fig. 2 displays the frequency dependence of the shear modulus of $(\mathrm{Ce{-}Cu})_{90}{-}\mathrm{Al}_{10}$ alloy for different temperatures. Trends were the same in the bulk metallic glasses containing iron. The position of the peak in G'' or onset of the G' decrease are shifted towards higher temperature when the frequency is increased from 0.01 to 1 Hz. All the curves can be superimposed by a horizontal allowing to get a master curve. Fig. 3 displays the curve associated to the loss modulus. The shifted data points now extend over approximately six orders of magnitude. The time–temperature superposition principle can be applied in the three different tested alloys. Since the temperature of the main transition (T_α) depends on the studied glass, the temperature has been normalized. It can be shown that the corresponding shift factor (not given here) obeys to an apparent Arrhenius behavior. The corresponding value of the apparent activation energy is $E_A = 2.3$ eV in the three alloys. This fairly high value may be attributed to the collective motion of a large number of

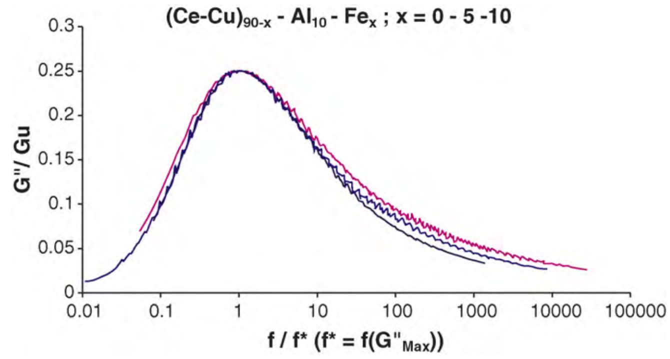

Fig. 3. Master curves for the loss modulus.

atoms [18,21–23] (see below for a brief discussion). This collective movements was described elsewhere described using the physical model introduced by Perez et al. [23–25], based on the concept of quasi-point defects initially developed in amorphous polymers and extrapolated to BMG [20].

Compared to results reported in other bulk metallic glasses, some common features and some differences appear: both the modulus variations *vs* temperature or *vs* frequency are similar in all the investigated alloys (Zr-based, Mg-based, Pd-based BMG), leading to very similar master curves [10–20]. This analogy indicates that the physical mechanisms at the origin of this evolutions are probably the same and then the physical model proposed to describe the curves obtained in Pd-, Zr- or Mg-based bulk metallic glasses can probably be also applied in the studied Ce-based materials [20]. However, the apparent activation energy E_A is much lower in these rare earth based material than for instance in Zr-based amorphous materials (about 5 eV in a Zr-based glass [20]) and also lower than in Mg-based BMG (3.0 eV for instance in a MgCu–Y alloy [21]). But if we compare the glass transition temperature of these materials, a very large difference is also observed, in the same order: T_g in Ce-based materials is about 350–390 K, while in Zr-based BMG is often 650–700 K and Mg-based alloys are intermediate. This temperature is an indicator of the mobility in the amorphous state: the higher T_g, the lower the mobility. So, it could be concluded that T_g and E_A are connected, at least indirectly.

3.3. Crystallization process

Crystallization can occur either during a continuous heating or during an isothermal annealing. Let us first present results corresponding to a continuous heating with an average heating rate of 1 K/min. X-ray diffraction spectra were recorded each 2 K from 303 to 553 K and from 2θ between 20° and 40°. Fig. 4 displays the 3D spectra for the three different investigated alloys, with various iron contents. Several conclusions can be drawn from these spectra:

- The three studied alloys evolve from an amorphous state to a crystalline one and the onset of crystallization is fairly rapid.
- At the end of the heating, peaks are identical in the three alloys.
- The iron content affects the crystallization route. Fig. 5 displays the variation as a function of temperature of the 33.7° peak area: in the alloys containing iron, crystallization occurs mainly in a single step while in the glass without iron, the process seems more complex: some peaks are observed only at the end of the process (for instance close to 22° or to 31°), one is always observed (close to 34°), whereas some others move progressively (for instance near 30° and 33°) (Fig. 4).

Fig. 6 displays the final spectrum recorded in the alloy without iron. Many peaks are clearly revealed, suggesting the presence

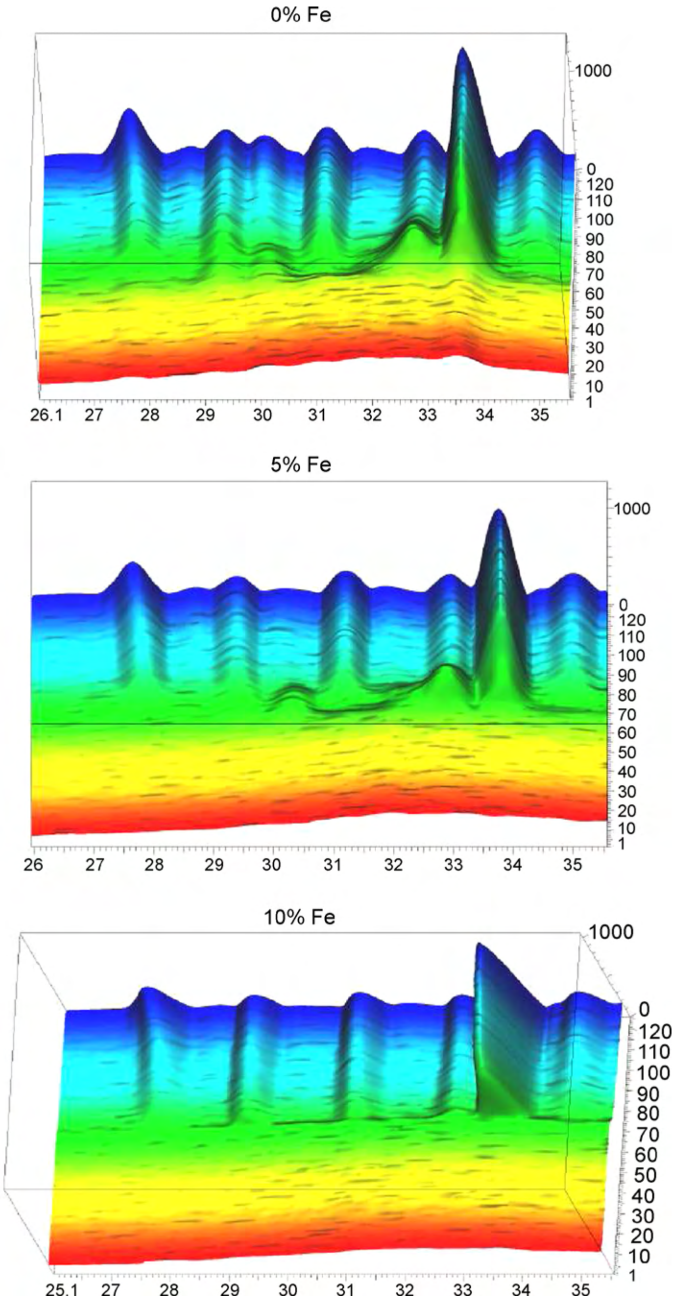

Fig. 4. X-ray diffraction spectra (3D representation) during continuous heating at 1 K/min, from 303 to 553 K. Angle range: 20–40°. (a) $x = 0\%$ Fe, (b) $x = 5\%$ Fe, (c) $x = 10\%$ Fe.

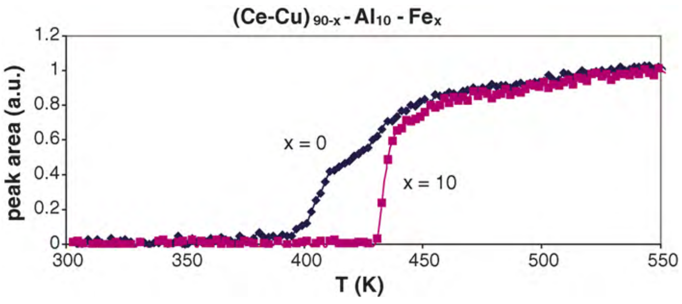

Fig. 5. Diffraction peak area *vs* time during continuous heating at 1 K/min in $(Ce–Cu)_{80}–Al_{10}–Fe_{10}$ BMG ($x = 0\%$ and $x = 10\%$) (peak at 33.7°).

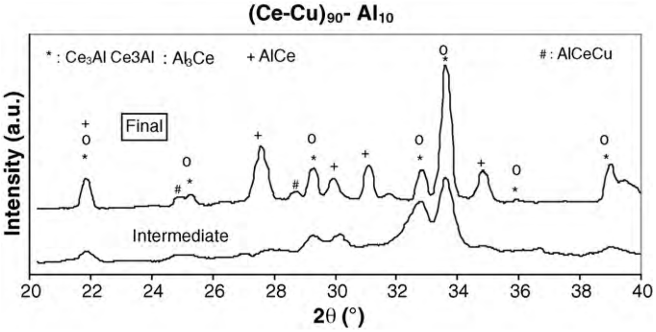

Fig. 6. XRD spectrum in $(Ce–Cu)_{90}–Al_{10}$, after heating at 403 and 553 K.

of various crystalline phases, in varying proportions. These phases were identified as mainly Ce_3Al (JCPDS 09-0268), Al_3Ce (JCPDS 29-0012), AlCe (JCPDS 31-0005) and AlCeCu (JCPDS 21-751). In practice, Cu and Fe are probably in solid solution in these phases.

Fig. 6 displays also an intermediate spectrum, obtained after heating up to 403 K for the same glass. Identification of the peaks is not easy, probably due to the existence of intermediate metastable phases. All Bragg crystalline peaks present in the intermediate spectrum also appear in the final XRD pattern, but the number of Bragg crystalline peaks in the final XRD pattern is more than that of intermediate spectrum. If the intermediate XRD spectrum consists of peaks from the crystalline phase superimposed on the diffuse maximum of remaining amorphous phase, the crystallization mode of the Fe-free Ce BMG can, therefore, be referred to the primary crystallization one: amorphous phase α — (primary crystallization) → amorphous phase α′ + primary crystalline phases — (secondary crystallization of remaining amorphous phase α′) → primary + secondary stable crystalline phases. However, TEM observation needs to be performed to identify the existence of remaining amorphous phase in the sample heated up to a temperature, e.g. 403 K. Such investigation is now in progress.

3.4. Relation between crystallization and dynamic modulus

Fig. 1 illustrated in a clear way that onset of crystallization induced a drastic increase of the storage modulus G'. Using the quantitative data reported in Section 3, it is now possible to connect the volume fraction of crystalline particles and the elastic modulus, either during a continuous heating or during an isothermal annealing. Figs. 7 and 8 display this parallel evolution in the alloy containing 10% of iron, where the crystallization kinetics is relatively simple. The volume fraction was estimated using the area below the main diffraction peak. The magnitude is expressed using arbitrary units. A good correlation between these two variations can be observed, suggesting that the increase in elastic modulus is closely connected to the quantity of crystalline phase.

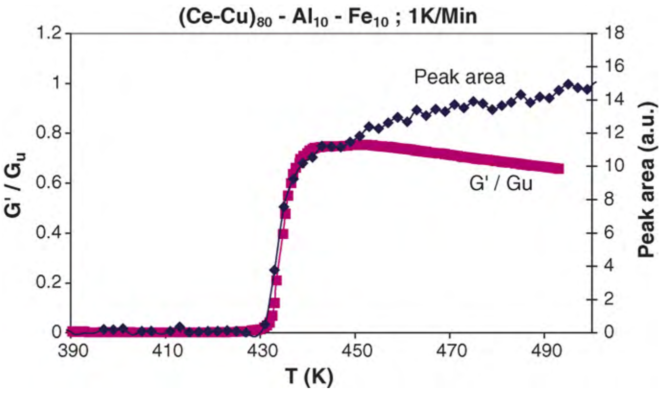

Fig. 7. Storage modulus and diffraction peak area *vs* temperature during continuous heating at 1 K/min in a $(Ce–Cu)_{80}–Al_{10}–Fe_{10}$ BMG.

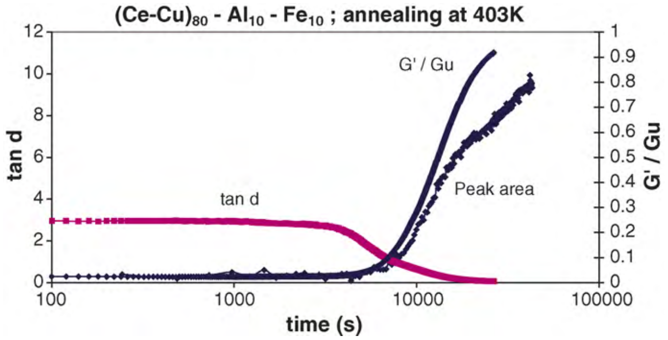

Fig. 8. Storage modulus, loss factor ($\tan\delta = G''/G'$) and diffraction peak area *vs* time during isothermal annealing at 403 K in a $(Ce–Cu)_{80}–Al_{10}–Fe_{10}$ BMG.

The size of the crystalline particles size can be roughly estimated using the Scherer formula. In this framework, the average particle size Φ of the diffracting particles is determined using the full width at half maximum (FWHM) of a diffraction peak occurring at 2θ. It is usually assumed that $\Phi = k/(\Delta(2\theta)\cos\theta)$, where $\Delta(2\theta)$ is the corresponding FWHM and k a numerical factor, frequently taken as $k = 0.9$. This formula has a physical meaning only for isotropic particles and when the contribution of the experimental device can be correctly withdrawn or neglected. In the present case, this correction is negligible (lower than 0.02°) and it may be assumed that crystalline particles, occurring in an isotropic medium, are mainly isotropic. This last assumption is supported by TEM observation reported in various BMG [10]. As soon as crystalline particles are detected, the corresponding, FWHM is about 0.5°, which corresponds to an average size of about 18 nm. Thus it can be concluded that crystallization progresses mainly by formation of new crystalline particles and not by the growth of existing ones. Results are independent on the used diffraction peak.

Similar results are obtained during an isothermal heating (Fig. 8), confirming therefore the good correlation between crystallinity and elastic features.

4. Conclusions

Measurements of dynamic shear modulus in large temperature and frequency ranges have been performed in three Ce-based bulk metallic glass, with various iron contents (between 0 and 10%). During a continuous heating a main relaxation is observed, which corresponds to a dynamic glass transition. The temperature of this transition is shifted towards higher temperature when the testing frequency is increased (for a given alloy), or when the iron content is increased (for a given testing frequency). The high value of the activation energy of this thermo-mechanically activated phenomenon ($E_A = 2.3$ eV) indicates that collective movements of atoms are involved in this relaxation. Annealing at high temperature, either during a continuous heating or during an isothermal annealing, induces a crystallization phenomenon. Formation of nano-crystalline particles induces a large increase of the storage modulus and a decrease of the loss modulus. X-ray diffraction experiments revealed that the crystallization process seems to be simplified when iron is present and that the elastic modulus increase is strongly connected to the volume fraction of crystalline particles.

Acknowledgements

The authors are grateful to the financial support of the Rhône-Alpes and Shanghai in the framework of the ARCUS program between France and China, Natural Science Foundation of China (Grant Nos: 50571055 and 50731008) and the Hong Kong Polytechnic University under Grant No. F-HK 15/08T.

References

[1] B. Zhang, M.X. Pan, D.Q. Zhao, W.H. Wang, Appl. Phys. Lett. 85 (2004) 61.
[2] B. Zhang, R.J. Wang, D.Q. Zhao, M.X. Pan, W.H. Wang, Phys. Rev. B 70 (2004) 224208.
[3] Q. Luo, B. Zhang, D.Q. Zhao, R.J. Wang, M.X. Pan, W.H. Wang, Appl. Phys. Lett. 88 (2006) 151915.
[4] Y.X. Wei, B. Zhang, R.J. Wang, M.X. Pan, D.Q. Zhao, W.H. Wang, Scripta Mater. 54 (2006) 599.
[5] B. Zhang, D.Q. Zhao, M.X. Pan, R.J. Wang, W.H. Wang, Acta Mater. 54 (2006) 3025.
[6] W.H. Wang, Prog. Mater. Sci. 52 (2007) 540.
[7] Z. Bian, A. Inoue, Mat. Sci. Eng., A 449–451 (2007) 114.
[8] W.H. Wang, J. Appl. Phys. 99 (2006) 093506.
[9] P. Yu, R.J. Wang, D.Q. Zhao, H.Y. Bai, Appl. Phys. Lett. 91 (2007) 201911.
[10] W.H. Li, K. Shin, C.G. Lee, B.C. Wei, T.H. Zhang, Appl. Phys. Lett. 90 (2007) 171928.
[11] J.M. Pelletier, B. Van de Moortèle, J. Non-Cryst. Solids 325 (2003) 133.
[12] O.P. Bobrov, V.A. Khonik, S.N. Laptev, M.Y. Yazvitsky, Scripta Mater. 49 (2003) 255.
[13] V.I. Belayavskii, O.P. Bobrov, A.T. Kosilov, V.A. Khonik, Phys. Stat. Sol. 38 (1996) 16.
[14] R. Scarfone, H.R. Sinning, J. Alloy Compd. 310 (2000) 229.
[15] D.N. Perera, A.P. Tsai, J. Phys. D: Appl. Phys. 32 (1999) 2933.
[16] A.V. Granato, J. Alloy Compd. 355 (2003) 171.
[17] D.N. Perera, A.P. Tsai, J. Phys.: Condens. Matter 11 (1999) 3029.
[18] K. Schröter, G. Wilde, R. Willnecker, M. Weiss, K. Samwer, E. Dontt, Eur. Phys. J. B5 (1998) 1.
[19] C. Gauthier, J.M. Pelletier, L. David, G. Vigier, J. Perez, J. Non-Cryst. Solid 274 (2000) 181.
[20] J.M. Pelletier, J. Alloy Compd. 393 (2005) 223.
[21] S. Puech, J.J. Blandin, J.L. Soubeyroux, Adv. Eng. Mater. 9 (2007) 764.
[22] S. Etienne, J.Y. Cavaillé, J. Perez, R. Point, M. Salvia, Rev. Sci. Instrum. 53 (1982) 1261.
[23] J. Perez, Physics and Mechanics of Amorphous Polymers, A.A. Belkema Publishers, Rotterdam (Netherlands), 1998.
[24] J.C. Cavaillé, J. Perez, J.P. Johari, J. Non-Crsyt. Solids 131–133 (1991) 935.
[25] M. Mangion, J.Y. Cavaillé, J. Perez, Philos. Mag., A 66 (1992) 773.